

RESEARCH

Open Access



Dysregulated arginine metabolism in precursor B-cell acute lymphoblastic leukemia in children: a metabolomic study

Wenqing Wang^{1,2†}, Liuting Yu^{2†}, Zhen Li¹, Yan Xiao², Hao Jiang⁴, Yan-lai Tang^{3*}, Yun Chen^{2*} and Hongman Xue^{1*}

Abstract

Background Precursor B-cell acute lymphoblastic leukemia (B-ALL) is the most common cancers in children. Failure of induction chemotherapy is a major factor leading to relapse and death in children with B-ALL. Given the importance of altered metabolites in the carcinogenesis of pediatric B-ALL, studying the metabolic profile of children with B-ALL during induction chemotherapy and in different minimal residual disease (MRD) status may contribute to the management of pediatric B-ALL.

Methods We collected paired peripheral blood plasma samples from children with B-ALL at pre- and post-induction chemotherapy and analyzed the metabolomic profiling of these samples by ultra-high performance liquid chromatography-mass spectrometry (UHPLC-MS). Healthy children were included as controls. We selected metabolites that were depleted in pediatric B-ALL and analyzed the concentrations in pediatric B-ALL samples. In vitro, we study the effects of the selected metabolites on the viability of ALL cell lines and the sensitivity to conventional chemotherapeutic agents in ALL cell lines.

Results Forty-four metabolites were identified with different levels between groups. KEGG pathway enrichment analyses revealed that dysregulated linoleic acid (LA) metabolism and arginine (Arg) biosynthesis were closely associated with pediatric B-ALL. We confirmed that LA and Arg were decreased in pediatric B-ALL samples. The treatment of LA and Arg inhibited the viability of NALM-6 and RS4;11 cells in a dose-dependent manner, respectively. Moreover, Arg increased the sensitivity of B-ALL cells to L-asparaginase and daunorubicin.

Conclusion Arginine increases the sensitivity of B-ALL cells to the conventional chemotherapeutic drugs L-asparaginase and daunorubicin. This may represent a promising therapeutic approach.

Keywords Precursor B-cell acute lymphoblastic leukemia, Minimal residual disease, Metabolomic profiling, Linoleic acid, Arginine

[†]Wenqing Wang and Liuting Yu contributed equally to this work.

*Correspondence:

Yan-lai Tang
tangylai@mail.sysu.edu.cn
Yun Chen
cheny653@mail.sysu.edu.cn
Hongman Xue
xuehm5@mail.sysu.edu.cn

Full list of author information is available at the end of the article



© The Author(s) 2024. **Open Access** This article is licensed under a Creative Commons Attribution-NonCommercial-NoDerivatives 4.0 International License, which permits any non-commercial use, sharing, distribution and reproduction in any medium or format, as long as you give appropriate credit to the original author(s) and the source, provide a link to the Creative Commons licence, and indicate if you modified the licensed material. You do not have permission under this licence to share adapted material derived from this article or parts of it. The images or other third party material in this article are included in the article's Creative Commons licence, unless indicated otherwise in a credit line to the material. If material is not included in the article's Creative Commons licence and your intended use is not permitted by statutory regulation or exceeds the permitted use, you will need to obtain permission directly from the copyright holder. To view a copy of this licence, visit <http://creativecommons.org/licenses/by-nc-nd/4.0/>.

Introduction

Acute lymphoblastic leukemia (ALL), one of the most common malignancies, has been reported to account for nearly one-third of all pediatric cancers [1]. According to immunophenotype classification, 85% of all cases of pediatric ALL belong to the Precursor B-cell acute lymphoblastic leukemia (B-ALL) [2]. Despite considerable advances in the treatment of pediatric B-ALL, a high mortality rate has been witnessed among children with relapsed or refractory cancer [3]. Therefore, novel therapeutic approaches and strategies are needed to further improve the prognosis of B-ALL and reduce side effects.

Minimal residual disease (MRD) refers to the presence of leukemia cells in the bone marrow and, less commonly, in the peripheral blood following chemotherapy, immunotherapy, or radiotherapy [4]. Compared to morphological assessment alone, MRD can better estimate the reduction in disease burden following treatment. Therefore, MRD has emerged as a crucial biomarker for risk stratification and individual risk-guided treatment decisions in B-ALL [5].

Recently, the application of different metabolomic approaches has been highly efficient in identifying novel mechanisms of disease pathogenesis and progression. Furthermore, significant metabolic alterations have been identified in several solid tumors and hematological malignancies, such as colorectal cancer [6], myeloma [7], chronic myelogenous leukemia [8], and acute myeloid leukemia [9]. However, the MRD status of pediatric B-ALL following induction chemotherapy hasn't been reported up to now. Studying the specific metabolic profile can be highly effective in understanding the causes of poor outcomes and providing insights into disease biology and mechanisms underlying drug resistance [10].

Amino acids are important sources of energy for malignant cells, and alterations in amino acid metabolism are associated with immunosuppressive properties of the tumor microenvironment [11]. It may be a promising strategy for tumor therapy to adjust amino acid metabolism and alter the nutrient content of the tumor microenvironment. Studies have shown that Arg can be used as a sensitizer for radiotherapy, with nearly 78% of patients with glioblastoma metastases gained achieving or partial remission when given arginine administration before radiotherapy [12]. Moreover, arginine directly inhibited lymphoma cell growth in vitro [13], as well as Enhances anti-tumour effects in breast cancer mice by improving immune status [14]. Arg malnutrition in leukaemia and lymphoma in vivo is often associated with Arg synthase deficiency [15]. Targeting abnormal arginine metabolism may help treat B-ALL in children.

In the present study, we assessed the association of MRD status with different metabolites following induction chemotherapy in pediatric B-ALL. It turned out that linoleic acid (LA) metabolism and arginine were associated with pediatric B-ALL. In vitro, LA and Arg inhibited the viability of NALM-6 and RS4;11 cells significantly. Furthermore, we found that treatment of arginine increased the sensitivity of B-ALL cells to conventional chemotherapeutic agents. Therefore, the application of LA and Arg can be a promising therapeutic option for pediatric B-ALL in the future.

Materials and methods

Study population

We enrolled 10 pediatric patients with B-ALL, of whom 5 patients (cohort A) were MRD (-) and 5 patients (cohort B) were MRD (+) at post-induction. Here, we selected leukemic blasts >5% as the cut-off value for MRD positivity and <0.01 for MRD negativity after induction. In addition, 5 healthy children were included as controls. The basic characteristics of the children with B-ALL and the induction chemotherapy regimen are summarised in Supplementary Tables 1 and 2. The study was conducted according to the guidelines of the Declaration of Helsinki, and approved by the Ethics Committee of Sun Yat-sen University (KY-2022-020-01). All participants under 16 years old provided written informed consents from parents or legal guardians. Samples were collected at the Affiliated Hospital of Sun Yat-sen University, and all children with B-ALL were treated according to the South China Collaborative Group for the Treatment of Pediatric ALL 2016 protocol (SCCCG-2016-ALL), where induction chemotherapy included prednisone trial, VDLD induction and CAM intensification. In our study, we mainly assessed MRD on day 26 after VDLD chemotherapy (post-induction).

Sample collection and preparation

Peripheral blood samples were collected from each subject at two time points: (1) at diagnosis (pre-induction) on day 0 and (2) after VDLD chemotherapy (post-induction) on day 26. In total, 3mL of peripheral venous whole blood was collected to ethylenediaminetetraacetic acid (EDTA) anticoagulant tubes from each participants who had not consumed any food or water. The samples were centrifuged at 2000 rpm for 10 min at 4 °C, and the collected supernatant was stored at -80 °C. All plasma samples were thawed on ice, following which 50 µL of each sample was transferred to a 1.5 mL polypropylene tube. It was mixed with 150 µL of methyl alcohol by vortexing for 10 min. Next, the mixture was centrifuged at 14,000 rpm for 10 min. The supernatants were transferred to another 1.5 mL polypropylene tube, dried

with nitrogen, and subsequently dissolved in 80 μL of a 1:1 mixture of methanol and ultrapure water. The samples were vortexed for 5 min and separated by centrifugation at 14,000 rpm for 10 min. The QC sample was prepared by mixing an equal aliquot of the supernatant from all of samples. Finally, supernatants were transferred to autosampler vials.

Metabolomics platform

Metabolomic profiling was performed on a Q Exactive Plus Hybrid Quadrupole-Orbitrap Mass Spectrometer with Thermo Vanquish UHPLC (Thermo, MA, USA) at Bay Laboratory of Shenzhen. All plasma samples were analyzed in both positive ion (ESI+) and negative ion (ESI-) modes, with the mass range varying from 100 to 1000 m/z in the full scan mode. Separation was performed on an ACQUITY UPLC BEH C18, 2 μm column; the mobile phase A was 0.1% formic acid in water, and mobile phase B was acetonitrile. The column temperature was maintained at 25 $^{\circ}\text{C}$, and elution was performed at a flow rate of 400 $\mu\text{L}/\text{min}$. A total of 2 μL of the sample was injected for negative ions and 2 μL for positive ions.

Data processing

The raw data files were imported into Compound Discoverer 3.2, and the intensity of each ion was normalized to generate a data matrix consisting of the m/z value, retention time, and normalized peak area. The peak intensity values of each plasma sample were classified according to the above study group, followed by further analysis.

Metabolic pathway enrichment analysis

The peak intensity values of metabolites with highly different abundance in plasma samples were imported into the MetaboAnalyst. MetaboAnalyst generates integrated pathway enrichment and pathway topology analyses to study the functions of untargeted metabolites. Metabolite identifiers were converted to the synonyms listed in the Human Metabolome Database (HMDB 5.0) [16]. The pathway impact measures represented the sum of important measures of significant metabolites generated by topology analysis and normalized to important measures of all metabolites in the associated pathway. In addition, we used the KEGG database to map significant metabolites to the pathways of interest [17, 18].

ELISA

Peripheral plasma was collected on day 26 of induction chemotherapy from children with B-ALL, as well as from

healthy children as controls (Supplementary Table 1). Arginine concentrations were measured using the Human Arginine (Arg) ELISA KIT (Reed Biotech, Wu Han) according to the manufacturer's instructions.

Cell lines

Human B-ALL cell line NALM-6 (ATCC, CRL-3273) and ALL cell line RS4;11 (ATCC, CRL-1873) and human normal peripheral blood mononuclear cells (PBMC) were obtained from the Scientific Research Centre, The Seventh Affiliated Hospital, Sun Yat-sen University (Shenzhen, China). The cells were cultured in RPMI1640 medium containing 10% fetal bovine serum and 1% penicillin/streptomycin at 37 $^{\circ}\text{C}$ in a humidified atmosphere of 5% CO_2 .

Cytotoxicity assay

The cytotoxicity of LA, Arg and chemotherapeutics were assessed by the CCK8 assay. In 96-well plates, cells were treated with different concentrations of LA, Arg (0, 100, 200, 300, 400 and 500 μM) and Arg 300 μM in combination with different chemotherapeutics for 24 h and then 10 μL CCK8 (5 mg/mL) was added to each well. After the cells were incubated in a 37 $^{\circ}\text{C}$ incubator for 4 h, the absorbance value was detected at 450 nm by microplate reader, and the IC50 value was calculated. All of the solutions were adjusted to a pH of 7.4 and stored at 4 $^{\circ}\text{C}$.

Statistical analysis

The metabolomics data were analyzed using the online software MetaboAnalyst 5.0 [19]. The supervised Orthogonal Partial Least Squares Discriminant Analysis (OPLS-DA) model was used to assess metabolic changes between groups. To assess the risk of overfitting of the OPLS-DA model, 1000 permutation tests were performed. Pathway enrichment analyses were performed using the Kyoto Encyclopedia of Genomes (KEGG) database. Qualitative and quantitative differences between subgroups were analysed using χ^2 test or Fisher's exact test for categorical parameters, and Student's t-test or Mann-Whitney U test was used to compare the difference in two groups as appropriate. Differences in cell viability were expressed as means \pm SDs of triplicate experiments performed independently. P-value less than 0.05 was considered significant.

Results

Baseline characteristics and metabolite profiling

Plasma samples were collected from 10 pediatric patients newly diagnosed with B-ALL and five healthy volunteers of similar age from the same geographical

area as controls. The baseline characteristics of patients are shown in (Supplementary Table 1) All children with B-ALL were treated with chemotherapy according to the South China protocol, a schedule of administration and dosing in the induction chemotherapy regimen is shown in (Supplementary Table 2) Risk stratification revealed that the MRD(+) group consisted of two high-risk, one standard-risk, and two low-risk individuals, while the MRD(-) group consisted of one standard-risk and four low-risk individuals (Supplementary Table 3). A total of 2,988 features were identified in the plasma samples. We used HMDB to annotate 274 metabolites in the plasma and found that 31 metabolites significantly differed between healthy volunteers and children with B-ALL at diagnosis, whereas 13 metabolites markedly differed between children with B-ALL with varied MRD statuses after induction.

Metabolic alterations in pediatric B-ALL at pre-induction compared with healthy controls

Distinct clusters of metabolites were identified in the peripheral plasma of children with B-ALL at pre-induction (cohort A and cohort B) compared to control individuals, as seen in the discovery cohort by OPLS-DA (Fig. 1A, D) and PCA score plots (Supplementary Fig. 1A). We set up a model that contained metabolomic information by fitting OPLS-DA. We evaluated its accuracy to classify new samples through 1000 random permutation tests during cross-validation (Fig. 1B, E). The model was reliable since the goodness of fit (R₂) and predictive ability (Q₂) were both greater than 0.5 variable Importance in Projection (VIP) scores were used to plot the changes in the levels of the identified metabolites in B-ALL compared to healthy controls (Fig. 1C, F). Furthermore, considering the statistically significant differences and the importance of the variables in prediction, we plotted the fold change in levels of identified metabolites in B-ALL compared to healthy controls (Supplementary Fig. 1C). Taken together, children with B-ALL experience significant changes in the metabolome of their peripheral plasma. These changes may be associated with the pathogenesis of B-ALL.

Metabolic changes in distinct MRD status at post-induction in pediatric B-ALL

We also evaluated the metabolic changes of children with B-ALL in different MRD states at post-induction chemotherapy. Differential metabolites in the cohort A and cohort B at post-induction were indicated through OPLS-DA (Fig. 1G) and PCA score plots (Supplementary Fig. 1B), as previously mentioned. We also fitted the OPLS-DA model and verified its reliability by cross-validating the Q₂ and R₂ values (Fig. 1H). Additionally,

we used VIP scores (Fig. 1I) and volcano plots (Supplementary Fig. 1D) to illustrate the significance and impact of differential metabolites between the two groups. The results revealed that metabolic alterations in children with B-ALL MRD (+) at post-induction chemotherapy differed from those in MRD (-) patients.

Analysis of pathogenic metabolites in children with B-ALL at pre-induction

To identify metabolic phenotypes that were associated with the development of B-ALL, we compared metabolic changes in plasma samples from B-ALL and healthy controls by hierarchical cluster analysis (Fig. 2A). It turned out that 12 metabolites were elevated and 13 metabolites were significantly decreased in children with B-ALL compared to healthy controls. We categorised the top twenty metabolites (Supplementary Table 4) and found that the major alterations of metabolites in pediatric B-ALL were fatty acid metabolism and amino acid metabolism, which was confirmed by KEGG analysis (Fig. 3A).

Metabolite variation in pediatric B-ALL with different responses to induction therapy

To investigate metabolite changes in children with B-ALL with different efficacy after induction chemotherapy, we compared metabolic changes between the MRD (+) and MRD (-) groups by hierarchical cluster analysis (Fig. 2B). The results indicated that 10 metabolites appeared to be elevated and 11 metabolites appeared to be decreased in the MRD (-) group compared to the MRD (+) group. The top metabolites were categorized in Supplementary Table 5. To figure out the functional characteristics of these metabolites, we performed pathway enrichment analysis by KEGG and identified significantly enriched pathways. Among the pathways that were altered, the most changes were observed in the pathways associated with arginine and ether lipids (Fig. 3B).

Metabolic characterization of linoleic acid and arginine

Our study revealed significant differences in linoleic acid (LA) levels between pediatric B-ALL patients and healthy controls, as for arginine (Arg) levels after induction chemotherapy for pediatric B-ALL with different MRD status. The metabolic pathways of LA and Arg were significantly enriched in KEGG analysis. Therefore, we further analyzed the mass spectral patterns and the relative abundance of LA and Arg (Fig. 4A). The results demonstrated that LA was decreased in pediatric B-ALL patients compared to healthy children while Arg was reduced in the MRD (+) group compared to the MRD (-) groups. More importantly, the reduction of Arg in MRD (+) group was confirmed by ELISA. Besides, a notable decrease in

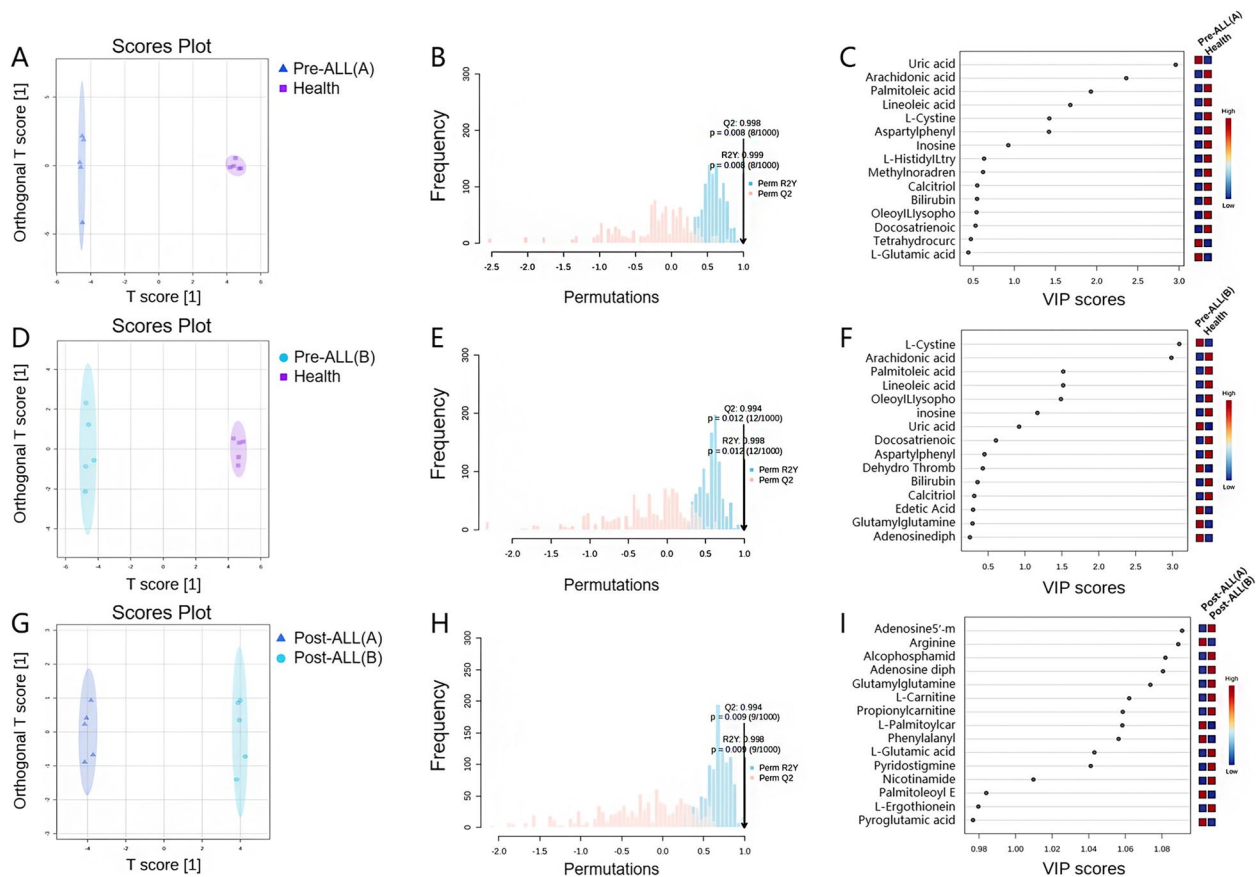


Fig. 1 Metabolic changes were observed in the peripheral plasma of pediatric B-ALL. **A, D** OPLS-DA score plots for comparison between healthy controls and pediatric B-ALL in cohort A and cohort B at pre-induction, respectively. **G** OPLS-DA score plots for comparison between cohort A and cohort B in B-ALL at post-induction. **B, E, H** The cross-validation results, tested with a permutation method repeated 1000 times. Both R2 and Q2 are greater than 0.5. **C, F** The VIP score plots for showing the impacts of differential metabolites in B-ALL compared to healthy controls. **I** The VIP score plots for showing the impacts of altered metabolites on MRD status after B-ALL induction chemotherapy

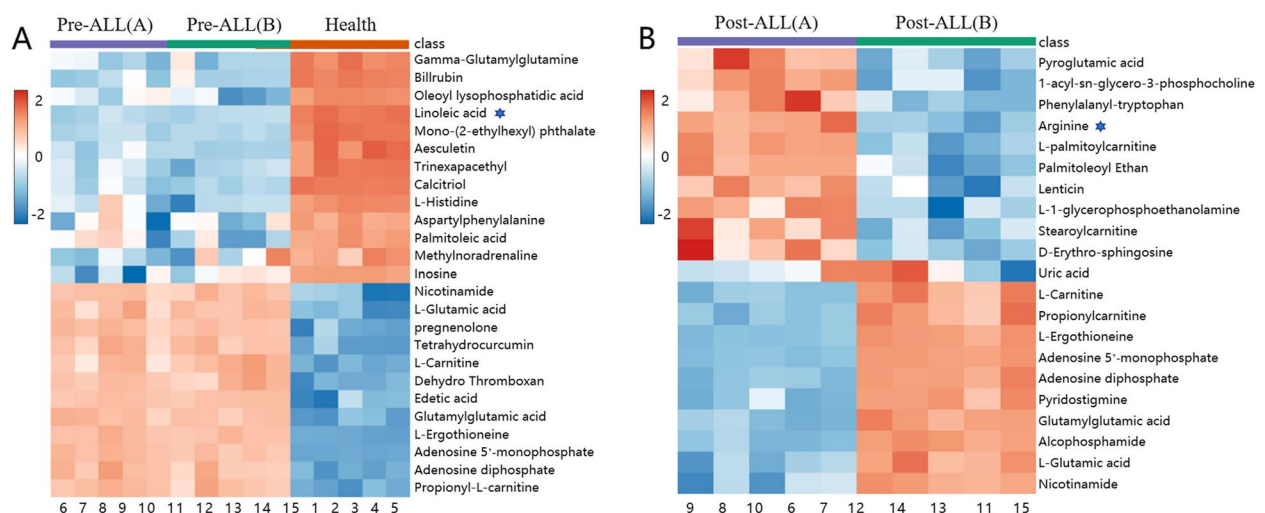


Fig. 2 The identification of pathogenic metabolites in pediatric B-ALL. Hierarchical cluster analysis was performed for metabolite differences in **(A)** children with B-ALL at pre-induction compared to healthy controls and **(B)** children with B-ALL of different MRD status at post-induction chemotherapy. The red color represents high relative concentrations of metabolites in each group, while the blue color represents low relative concentrations of metabolites in each group

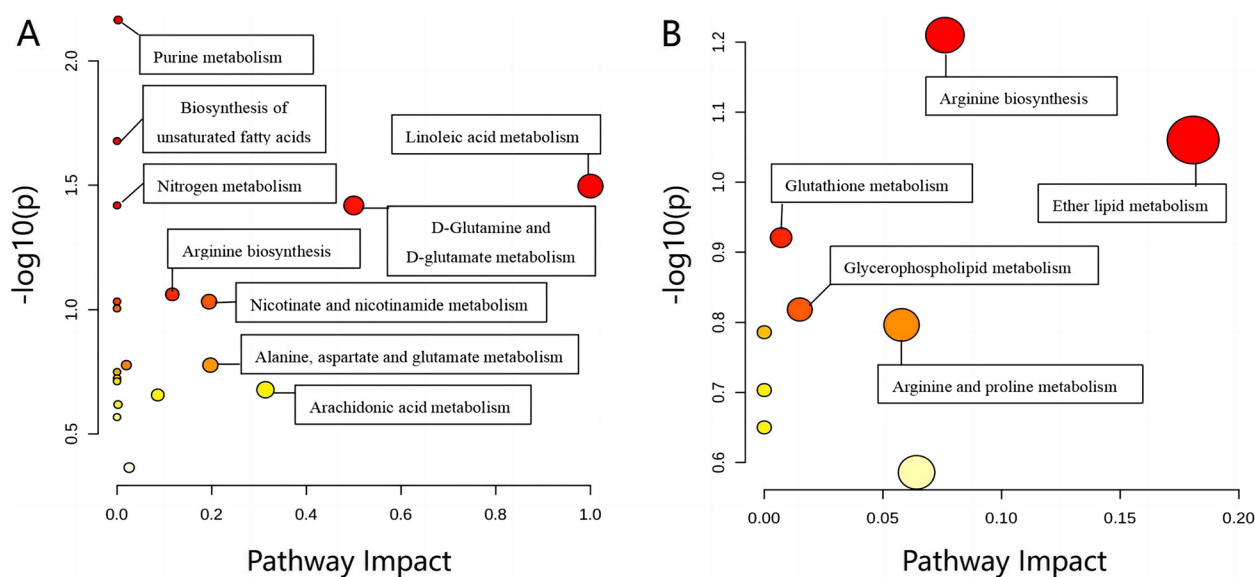


Fig. 3 KEGG pathway enrichment analysis. Significant changes of the metabolites were observed in **(A)** children with B-ALL at the time of diagnosis compared to healthy controls, and **(B)** children with B-ALL of different MRD status after induction chemotherapy

arginine levels was observed in children with B-ALL compared to healthy controls (Supplementary Fig. 2).

Linoleic acid and arginine inhibited the viability of ALL cell lines

Through evaluation the levels of metabolites in different groups, we found that linoleic acid (LA) and arginine (Arg) were significantly decreased in pediatric B-ALL compared to healthy controls in the discovery cohort at pre-induction and post-induction, respectively. To confirm the role of LA and Arg in ALL, the ALL cell lines were treated with LA and Arg, respectively. Compared to phosphate buffer saline (PBS), both LA and Arg remarkably inhibited cell viability in NALM-6 and RS4;11 cell lines in a dose-dependent manner (Fig. 5A) without negative effects on normal PBMC. These results indicated that LA and Arg exhibited anti-ALL activity with high specificity.

Arginine increased the sensitivity of ALL cells to conventional chemotherapeutic agents

As arginine levels were diverse in pediatric B-ALL patients with different MRD states following induction chemotherapy and arginine inhibited ALL cell viability in vitro, we wondered whether arginine could be used in combination with the most commonly used chemotherapeutics (VDLD) in B-ALL treatment. To this end, ALL cell lines NALM-6 and RS4;11 were treated with Arg in combination with chemotherapeutic agents for 24 h (i.e. dexamethasone, L-asparaginase, daunorubicin, vincristine). These agents were normally applied to treat

pediatric ALL patients. The results showed that combination of Arg and L-asparaginase (L-ASP) and daunorubicin (DNR) respectively at fixed molar combination ratios exert greater effects on inhibiting cell viability than that of L-ASP or DNR alone (Fig. 6A). Therefore, Arg could effectively increase the sensitivity of B-ALL cells to L-ASP and DNR.

Discussion

B-ALL has been reported as the most common pediatric cancer [20]. Although conventional chemotherapy contributes to disease-free survival in more than 85% of pediatric patients with ALL, survival after relapse is very poor. MRD, which is often used to study hematological cancer, serves as a primary indicator to assess relapsed ALL in a post-induction setting [21]. In recent years, researchers have recognized altered metabolism as a cornerstone mechanism underlying oncogenesis and a hallmark of cancer [22]. Furthermore, tumor metabolism represents a readily druggable molecular space for identifying vulnerable metabolic targets in tumors [23]. For instance, a metabolite with a causal effect on the disease indicates the possibility of the involvement of an enzyme in its biosynthetic pathway that could serve as a therapeutic target [24]. Therefore, metabolomic insights can pave the way toward discovering novel therapeutic strategies for B-ALL, especially for relapsed and refractory B-ALL.

In this study, we performed an in-depth metabolomic analysis of peripheral plasma from B-ALL children at pre-induction chemotherapy to determine the

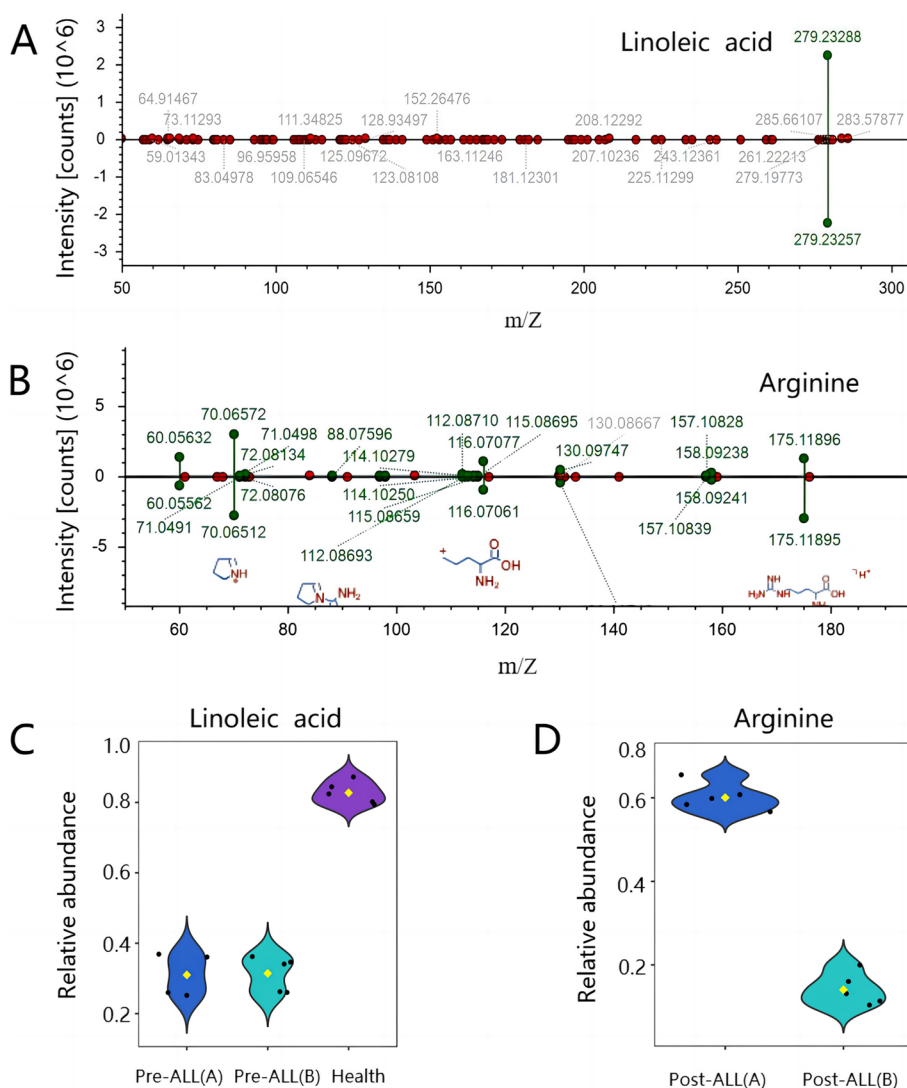


Fig. 4 The mass spectral patterns and the relative abundance of linoleic acid and arginine. **A-B** Fragmentation profiles of LA and Arg on MS, respectively. **C** Comparison of the relative abundance of linoleic acid between Cohort A and Cohort B at pre-induction and healthy controls. **D** Comparison of the relative abundance of Arg in cohort A and cohort B at post-induction in B-ALL.

differences in metabolites between B-ALL children and healthy subjects, as well as the differences in metabolites in B-ALL children with different MRD states at post-induction chemotherapy [25]. In total, 2988 metabolites were annotated in all collected samples, out of which 273 metabolites were best matched to the BioCyc [26], HMDB, or KEGG databases. Significant changes in the metabolomic composition of children with B-ALL were observed during induction chemotherapy. These observations suggested that metabolic reprogramming occurred in children with B-ALL to overcome inadequate nutrient supply and to generate the energy required for cell proliferation and survival. The metabolic reprogramming may

be a potential driver of hematological tumor pathogenicity in children with B-ALL.

The findings of this study indicate that the presence of peripheral blast cells exerts an influence on the metabolic activity of the organism. Firstly, a comparative analysis was conducted between the pre-induction B-ALL group and healthy controls, which revealed more pronounced alterations in fatty acid metabolism in children with ALL than in healthy controls. Furthermore, notable alterations in arginine metabolism were identified in patients with disparate MRD statuses following induction chemotherapy. Through comparison of samples of healthy controls and pediatric B-ALL patients at pre-induction, 31 metabolites were selected which showed significant enrichment

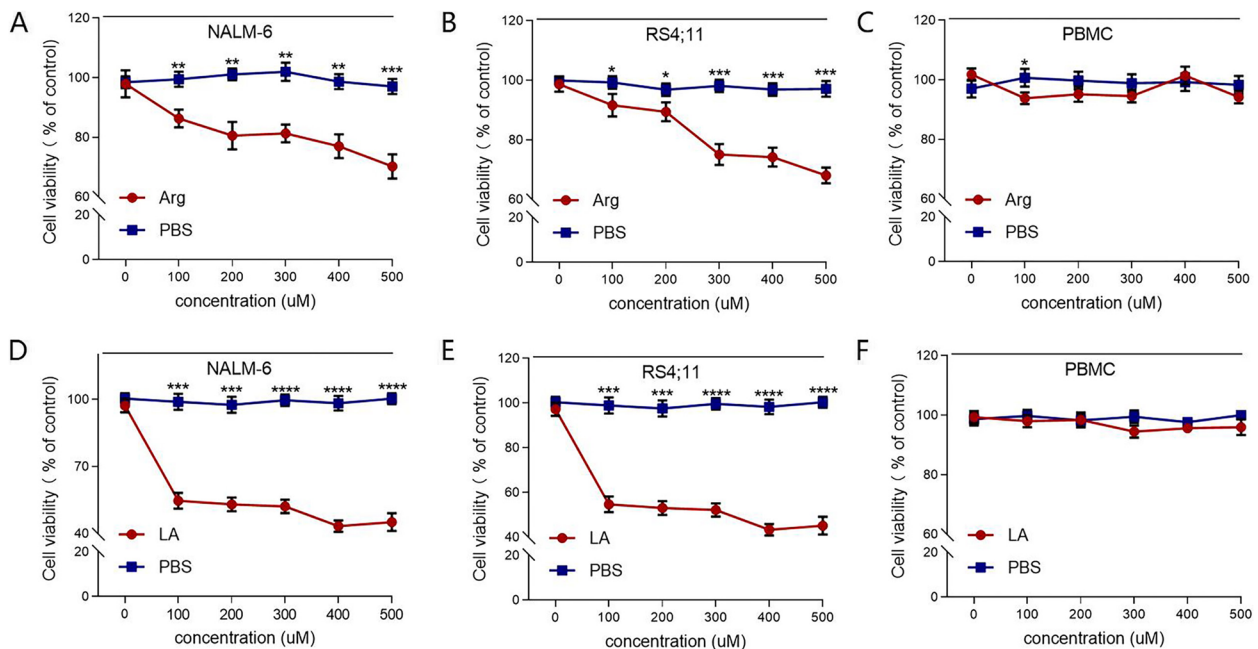


Fig. 5 LA and Arg inhibited the viability of ALL cell lines. **A-C** Arg and **(D-F)** LA inhibited the viability of NALM-6, RS4;11 cell lines rather than normal PBMC, as determined by CCK8 assay. Data are expressed as mean \pm SEM of three independent experiments. * $p < .05$, ** $p < .01$, *** $p < .001$, **** $p < .0001$

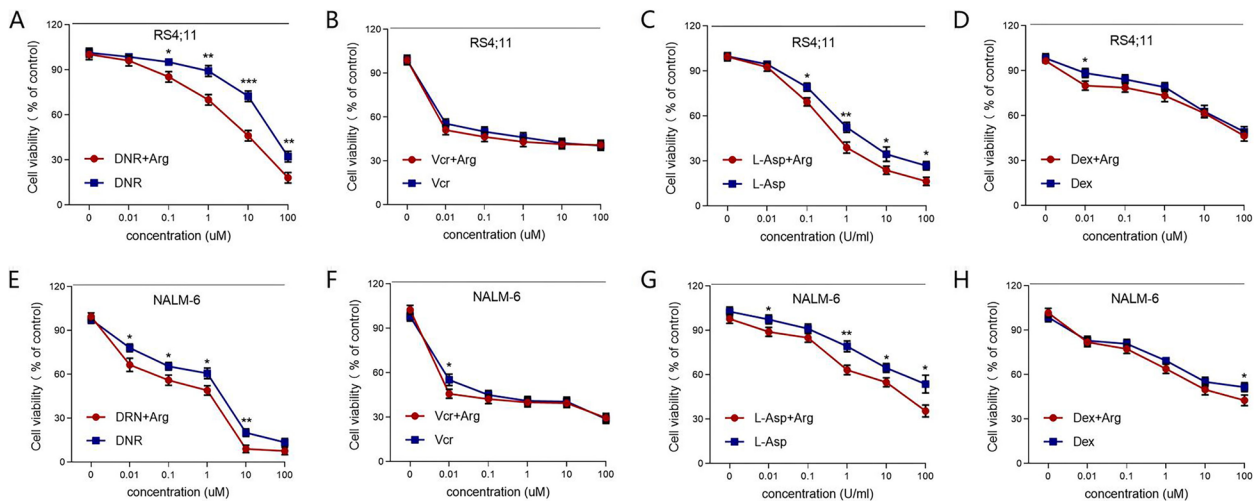


Fig. 6 Effects of Arg treatment alone and in combination with different chemotherapeutic drugs in (A-D) RS4;11 and in (E-H) NALM-6 cells. Cells were treated with indicated concentrations and fixed molar ratios and viability assessed by CCK8 assay after 24 h incubation. Data are expressed as mean \pm SEM of three independent experiments. * $p < .05$, ** $p < .01$, *** $p < .001$

for several processes, including LA metabolism, D-glutamine and D-glutamate metabolism, and nitrogen metabolism. Besides, 13 metabolites were identified with different levels in pediatric B-ALL samples with different MRD status post-induction. These metabolites exhibited distinct enrichment for processes including arginine metabolism, ether- lipid metabolism and glutathione

metabolism. Dysregulation of fatty acid and amino acid metabolism, particularly glutamine, serine, and glycine, has been reported to support the growth of cancer cells [27]. Aberrant regulation of amino acids and extracellular matrix (ECM) has been known to promote pro-tumor activity [28]. The functions of these newly identified differential metabolites need to be further investigated.

Of interest, two depleted metabolites LA and Arg were observed during induction chemotherapy. The reduction of LA and Arg in the peripheral blood of pediatric B-ALL patients indicated that they played as a potential protective role in B-ALL progression. LA is an n-6 polyunsaturated fatty acid [29], which is enzymatically oxidized to different derivatives involved in cell signaling [30]. It inhibited colorectal cancer cell growth by inducing apoptosis [31]. Supplementation of LA has been a potential adjuvant treatment for breast cancer [32, 33]. Long-term treatment of cancer cells with LA induced a dormancy-like phenotype [34]. However, LA has not been used as a treatment option for leukemia. In this regard, our work provides a new link between altered LA metabolism and B-ALL pathogenesis. Amino acids play crucial roles in cancer progression beyond their function as building blocks for protein synthesis [35]. Arg is a semi-essential amino acid that is involved in immune regulation. Arg-derived NO activated cytotoxic T cells [36] and macrophages [37], thus promoting the immune response against tumor cells. Geiger Roger et al. reported that arginine revealed anti-tumor activity by enhancing the proliferation, differentiation and survival of T cells [38]. Engineered bacteria can produce lots of arginine when implanted into tumor and exhibit synergistic effects with PD-L1 blockers on augmenting the infiltration of cytotoxic T cells and decreasing the infiltration of Treg cells in the tumor [39]. In addition, Arg was reported to inhibit the growth of gastric cancer cells [40] and mice melanoma cells [41]. The administration of arginine enhanced the therapeutic effects of radiation in patients with brain metastases [42].

Arginine depletion has been shown to be effective in the treatment of tumours [43–45]. Such as, arginine depletion using BCT-100 a pegylated (PEG) recombinant human arginase reduced disease burden and enhanced the survival in ALL murine xenografts [46]. However, our study suggests that high levels of Arg may increase the response of B-ALL cells to induction chemotherapy. This is similar to some studies suggesting that arginine may enhance anti-tumour activity. [38, 40, 41, 47]. Given the limitations of the current study, further research is required to investigate the implications for the underlying molecular mechanisms of arginine in pediatric B-ALL.

However, this study has a few limitations. Firstly, the fusion genes in the sample were diverse and it was not possible to observe the effect of a particular fusion gene on metabolism in isolation. Secondly, the study did not include patients whose end-of-induction MRD levels ranged from 0.01 to 5%. In addition, we used a small sample size and although several significant findings were identified, a larger sample size may have revealed additional differences.

Therefore, we may miss some potentially relevant metabolites. Larger-scale functional studies *in vivo* and *in vitro* are needed to determine the relationship between metabolic alterations and children with B-ALL.

Conclusions

Overall, the present study identified novel metabolic alterations in children with B-ALL by performing metabolomic analysis of peripheral blood before and after induction chemotherapy. Our findings indicate that Arg is deficient in B-ALL and that increasing arginine may potentially enhance the response of B-ALL cells to induction chemotherapy. Therefore, targeting Arg in chemotherapy may help treat children with B-ALL.

Abbreviations

B-ALL	Precursor B-cell acute lymphoblastic leukemia
MRD	Minimal residual disease
UHPLC-MS	Ultra-high performance liquid chromatography-mass spectrometry
LA	Linoleic acid
Arg	Arginine
OPLS-DA	Orthogonal partial least squares discriminant analysis
VIP	Variable Importance in Projection
KEGG	Kyoto encyclopedia of genomes
L-ASP	L-asparaginase
DNR	Daunorubicin
ECM	Extracellular matrix

Supplementary Information

The online version contains supplementary material available at <https://doi.org/10.1186/s12887-024-05015-3>.

Supplementary Material 1.

Supplementary Material 2.

Acknowledgements

Not applicable.

Authors' contributions

Conceptualization, W.W. and Y.C.; methodology, W.W.; software, Y.X.; validation, W.W., Z.L.; Y.X. and H.J.; resources, Y.T. and Z.L.; data curation, W.W.; original draft preparation, W.W. and L.Y.; review and editing, Y.C.; L.Y. and H.X.; supervision, Y.C. and H.X.; All authors have read and agreed to the published version of the manuscript.

Funding

This study was supported by Shenzhen Science and Technology Innovation Commission (JCYJ 20190809160609727); Sanming Project of Medicine in Shenzhen (SZSM202011004).

Availability of data and materials

The raw data used to support the findings of this study are available from the corresponding author upon reasonable request.

Declarations

Ethics approval and consent to participate

The study was approved by the Institutional Review Board of The Seventh Affiliated Hospital of Sun Yat-Sen University. All participants under 16 years old provided written informed consents from parents or legal guardians. The data presented in this study are available in the article.

Consent for publication

Not applicable.

Competing interests

The authors declare no competing interests.

Author details

¹Pediatric Hematology Laboratory, Division of Hematology/Oncology, Department of Pediatrics, The Seventh Affiliated Hospital of Sun Yat-Sen University, Shenzhen, Guangdong 518107, China. ²Edmond H. Fischer Translational Medical Research Laboratory, Scientific Research Center, The Seventh Affiliated Hospital, Sun Yat-sen University, Shenzhen, Guangdong 518107, China. ³Department of Pediatrics, The First Affiliated Hospital, Sun Yat-sen University, Guangzhou, Guangdong 510080, China. ⁴Medical laboratory science, The Seventh Affiliated Hospital of Sun Yat-Sen University, Shenzhen, Guangdong 518107, China.

Received: 2 April 2024 Accepted: 14 August 2024

Published online: 22 August 2024

References

- Paidi SK, Raj P, Bordett R, Zhang C, Karandikar SH, Pandey R, Barman I. Raman and quantitative phase imaging allow morpho-molecular recognition of malignancy and stages of B-cell acute lymphoblastic leukemia. *Biosens Bioelectron.* 2021;190:113403.
- Jedraszka K, Malczewska M, Parysek-Wojcik K, Lejman M. Resistance mechanisms in pediatric B-cell acute lymphoblastic leukemia. *Int J Mol Sci.* 2022;23(6).
- Black KL, Naqvi AS, Asnani M, Hayer KE, Yang SY, Gillespie E, Bagashev A, Pillai V, Tasian SK, Gazzara MR, et al. Aberrant splicing in B-cell acute lymphoblastic leukemia. *Nucleic Acids Res.* 2018;46(21):11357–69.
- Kruse A, Abdel-Azim N, Kim HN, Ruan Y, Phan V, Ogana H, Wang W, Lee R, Gang EJ, Khazal S, et al. Minimal residual disease detection in acute lymphoblastic leukemia. *Int J Mol Sci.* 2020;21(3).
- Cheng S, Inghirami G, Cheng S, Tam W. Simple deep sequencing-based post-remission MRD surveillance predicts clinical relapse in B-ALL. *J Hematol Oncol.* 2018;11(1):105.
- Wang Y, Hinz S, Uckermann O, Honscheid P, von Schonfels W, Burmeister G, Hendricks A, Ackerman JM, Baretton GB, Hampe J, et al. Shotgun lipidomics-based characterization of the landscape of lipid metabolism in colorectal cancer. *Biochim Biophys Acta Mol Cell Biol Lipids.* 2020;1865(3):158579.
- Huang HY, Wang Y, Wang WD, Wei XL, Gale RP, Li JY, Zhang QY, Shu LL, Li L, Li J, et al. A prognostic survival model based on metabolism-related gene expression in plasma cell myeloma. *Leukemia.* 2021;35(11):3212–22.
- de Almeida FC, Berzoti-Coelho MG, Toro DM, Cacemiro M, Bassan VL, Barretto GD, Garibaldi P, Palma LC, de Figueiredo-Pontes LL, Sorgi CA, et al. Bioactive lipids as chronic myeloid leukemia's potential biomarkers for disease progression and response to tyrosine kinase inhibitors. *Front Immunol.* 2022;13:840173.
- Idle JR, Seipel K, Bacher U, Pabst T, Beyoglu B. (2R,3S)-dihydroxybutanoic acid synthesis as a novel metabolic function of mutant isocitrate dehydrogenase 1 and 2 in acute myeloid leukemia. *Cancers.* 2020;12(10):2842.
- Stockard B, Garrett T, Guingab-Cagmat J, Meshinchi S, Lamba J. Distinct metabolic features differentiating FLT3-ITD AML from FLT3-WT childhood acute myeloid leukemia. *Sci Rep-UK.* 2018;8(1):5534.
- Liao P, Chang N, Xu B, Qiu Y, Wang S, Zhou L, He Y, Xie X, Li Y. Amino acid metabolism: challenges and opportunities for the therapeutic treatment of leukemia and lymphoma. *Immunol Cell Biol.* 2022;100(7):507–28.
- Al-Waili NS, Butler GJ. A combination of radiotherapy, nitric oxide and a hyperoxygenation sensitizing protocol for brain malignant tumor treatment. *Med Hypotheses.* 2007;68(3):528–37.
- Shu XL, Liu XL, Zhong JX, Liu J. L-arginine enhances arginine deiminase induced human lymphoma cell growth inhibition through NF- κ Bp65 and p53 expression in vitro. *Eur Rev Med Pharmacol.* 2014;18(15):2124–31.
- Cao Y, Wang Q, Du Y, Liu F, Zhang Y, Feng Y, Jin F. L-arginine and docetaxel synergistically enhance anti-tumor immunity by modifying the immune status of tumor-bearing mice. *Int Immunopharmacol.* 2016;35:7–14.
- Keshet R, Erez A. Arginine and the metabolic regulation of nitric oxide synthesis in cancer. *Dis Model Mech.* 2018;11(8):dmm033332.
- Wishart DS, Guo A, Oler E, Wang F, Anjum A, Peters H, Dizon R, Sayeeda Z, Tian S, Lee BL, et al. HMDB 5.0: the human metabolome database for 2022. *Nucleic Acids Res.* 2022;50(D1):D622–31.
- Kanehisa M, Sato Y, Kawashima M, Furumichi M, Tanabe M. KEGG as a reference resource for gene and protein annotation. *Nucleic Acids Res.* 2016;44(D1):D457–62.
- Kanehisa M, Furumichi M, Tanabe M, Sato Y, Morishima K. KEGG: new perspectives on genomes, pathways, diseases and drugs. *Nucleic Acids Res.* 2017;45(D1):D353–61.
- Yao M, Yang Z, Rong X, Hu X, Yao N, Zhu M, Wang X, Zhu X, Yin J. The exploration of fetal growth restriction based on metabolomics: a systematic review. *Metabolites.* 2022;12(9):860.
- Guo M, Rever J, Nguyen P, Akella NM, Reid G, Maxwell CA. Centrosome amplification is a potential molecular target in paediatric acute lymphoblastic leukemia. *Cancers.* 2022;15(1):154.
- Chiaretti S, Messina M, Della SI, Picocchi A, Cafforio L, Cavalli M, Taherinasab A, Ansuinelli M, Elia L, Albertini PG, et al. Philadelphia-like acute lymphoblastic leukemia is associated with minimal residual disease persistence and poor outcome. First report of the minimal residual disease-oriented GIMEMA LAL1913. *Haematologica.* 2021;106(6):1559–68.
- Zhu Y, Gu L, Lin X, Liu C, Lu B, Cui K, Zhou F, Zhao Q, Prochowick EV, Fan C, et al. Dynamic regulation of ME1 phosphorylation and acetylation affects lipid metabolism and colorectal tumorigenesis. *Mol Cell.* 2020;77(1):138–49.
- Hunger SP, Raetz EA. How I treat relapsed acute lymphoblastic leukemia in the pediatric population. *Blood.* 2020;136(16):1803–12.
- Rashkovan M, Ferrando A. Metabolic dependencies and vulnerabilities in leukemia. *Gene Dev.* 2019;33(21–22):1460–74.
- Saito T, Wei Y, Wen L, Wolthers BO, Tsai CY, Harris MH, Stevenson K, Byersdorfer C, Oparaji JA, et al. Impact of acute lymphoblastic leukemia induction therapy: findings from metabolomics on non-fasted plasma samples from a biorepository. *Metabolomics.* 2021;17(7):64.
- Karp PD, Billington R, Caspi R, Fulcher CA, Latendresse M, Kothari A, Keseler IM, Krummenacker M, Midford PE, Ong Q, et al. The BioCyc collection of microbial genomes and metabolic pathways. *Brief Bioinform.* 2019;20(4):1085–93.
- Li Z, Zhang H. Reprogramming of glucose, fatty acid and amino acid metabolism for cancer progression. *Cell Mol Life Sci.* 2016;73(2):377–92.
- Kang YP, Ward NP, DeNicola GM. Recent advances in cancer metabolism: a technological perspective. *Exp Mol Med.* 2018;50(4):1–16.
- Szczuko M, Kikut J, Komorniak N, Bilicki J, Celewicz Z, Zietek M. The role of arachidonic and linoleic acid derivatives in pathological pregnancies and the human reproduction process. *Int J Mol Sci.* 2020;21(24):9628.
- Karpishev V, Nikkhoo A, Hojjat-Farsangi N, Namdar A, Azizi G, Ghalamfarsa G, Sabz G, Yousefi M, Yousefi B, Jadidi-Niaragh F. Prostaglandin E2 as a potent therapeutic target for treatment of colon cancer. *Prostag Oth Lipid M.* 2019;144:106338.
- Whelan J, Fritsche K. Linoleic acid. *Adv Nutr.* 2013;4(3):311–2.
- Ogata R, Mori S, Kishi S, Sasaki R, Iwata N, Ohmori H, Sasaki T, Nishiguchi Y, Nakashima C, Goto K, et al. Linoleic acid upregulates microRNA-494 to induce quiescence in colorectal cancer. *Int J Mol Sci.* 2021;23(1):225.
- McCrorie TA, Keaveney EM, Wallace JM, Binns N, Livingstone MB. Human health effects of conjugated linoleic acid from milk and supplements. *Nutr Res Rev.* 2011;24(2):206–27.
- Dilzer A, Park Y. Implication of conjugated linoleic acid (CLA) in human health. *Crit Rev Food Sci.* 2012;52(6):488–513.
- Jiang J, Batra S, Zhang J. Asparagine: a metabolite to be targeted in cancers. *Metabolites.* 2021;11(6):402.
- Tang K, Zhang H, Deng J, Wang D, Liu S, Lu S, Cui Q, Chen C, Liu J, Yang Z, et al. Ammonia detoxification promotes CD8(+) T cell memory development by urea and citrulline cycles. *Nat Immunol.* 2023;24(1):162–73.
- Dussold C, Zilinger K, Turunen J, Heimberger AB, Miska J. Modulation of macrophage metabolism as an emerging immunotherapy strategy for cancer. *J Clin Invest.* 2024;134(2).
- Geiger R, Rieckmann JC, Wolf T, Basso C, Feng Y, Fuhrer T, Kogadeeva M, Picotti P, Meissner F, Mann M, et al. L-Arginine modulates T cell metabolism and enhances survival and anti-tumor activity. *Cell.* 2016;167(3):829–42.

39. Canale FP, Basso C, Antonini G, Perotti M, Li N, Sokolovska A, Neumann J, James MJ, Geiger S, Jin W, et al. Metabolic modulation of tumours with engineered bacteria for immunotherapy. *Nature*. 2021;598(7882):662–6.
40. Shu XL, Xu H, Yu TT, Zhong JX, Lei T. Regulation of apoptosis in human gastric cancer cell line SGC-7901 by L-arginine. *Panminerva Med*. 2014;56(3):227–31.
41. Zhang J, Wang S, Guo X, Lu Y, Liu X, Jiang M, Li X, Qin B, Luo Z, Liu H, et al. Arginine supplementation targeting tumor-killing immune cells reconstructs the Tumor Microenvironment and enhances the Antitumor Immune Response. *ACS Nano*. 2022;16(8):12964–78.
42. Marullo R, Castro M, Yomtoubian S, Calvo-Vidal MN, Revuelta MV, Krumsiek J, Cho A, Morgado PC, Yang S, Medina V, et al. The metabolic adaptation evoked by arginine enhances the effect of radiation in brain metastases. *Sci Adv*. 2021;7(45):eabg1964.
43. Yau T, Cheng P, Chiu J, Kwok G, Leung R, Liu AM, Cheung TT, Ng CT. A phase 1 study of pegylated recombinant arginase (PEG-BCT-100) in combination with systemic chemotherapy (capecitabine and oxaliplatin) [PACOX] in advanced hepatocellular carcinoma patients. *Invest New Drug*. 2022;40(2):314–21.
44. Cheng P, Liu AM, Bessudo A, Mussai F. Safety, PK/PD and preliminary anti-tumor activities of pegylated recombinant human arginase 1 (BCT-100) in patients with advanced arginine auxotrophic tumors. *Invest New Drug*. 2021;39(6):1633–40.
45. Mussai F, De Santo C, Cheng P, Thomas IF, Ariti C, Upton L, Scarpa U, Stavrou V, Sydenham M, Burnett AK, et al. A randomised evaluation of low-dose Ara-C plus pegylated recombinant arginase BCT-100 versus low dose Ara-C in older unfit patients with acute myeloid leukaemia: results from the LI-1 trial. *Brit J Haematol*. 2023;200(5):573–8.
46. De Santo C, Booth S, Vardon A, Cousins A, Tubb V, Perry T, Noyvert B, Beggs A, Ng M, Halsey C, et al. The arginine metabolome in acute lymphoblastic leukemia can be targeted by the pegylated-recombinant arginase I BCT-100. *Int J Cancer*. 2018;142(7):1490–502.
47. Marigo I, Zilio S, Desantis G, Mlecnik B, Agnellini A, Ugel S, Sasso MS, Qualls JE, Kratochvill F, Zanovello P, et al. T Cell Cancer Therapy requires CD40-CD40L activation of Tumor Necrosis factor and inducible nitric-oxide-synthase-producing dendritic cells. *Cancer Cell*. 2016;30(3):377–90.

Publisher's note

Springer Nature remains neutral with regard to jurisdictional claims in published maps and institutional affiliations.